Amino Acids (2011) 40:453–465
DOI 10.1007/s00726-010-0657-5

ORIGINAL ARTICLE

The agmatine-degrading enzyme agmatinase: a key to agmatine signaling in rat and human brain?

H.-G. Bernstein · C. Derst · C. Stich · H. Prüss · D. Peters · M. Krauss · B. Bogerts · R. W. Veh · G. Laube

Received: 7 May 2010 / Accepted: 5 June 2010 / Published online: 20 June 2010

Abstract Agmatinase, an ureohydrolase belonging to the arginase family, is widely expressed in mammalian tissues including the brain. Here, it may serve two different functions, the inactivation of the arginine derivative agmatine, a putative neurotransmitter, and the formation of the diamine putrescine. In order to identify the cellular sources of agmatinase expression in the brain, we generated a polyclonal monospecific antibody against recombinant rat agmatinase. With immunocytochemistry, selected areas of rat and human brain were screened. Clearly, in both species agmatinase-like immunoreactivity was predominantly detected in distinct populations of neurons, especially cortical interneurons. Also, principal neurons in limbic regions like the habenula and in the cerebellum robustly expressed agmatinase protein. When comparing the overall agmatinase expression with immunocytochemical data available for agmatine and polyamine biosynthetic enzymes, the observed pattern may argue in favor of an agmatine inactivating function rather than fueling the alternative pathway of polyamine synthesis. The putative neurotransmitter agmatine is seemingly involved with mental disorders. Therefore, agmatinase may be similarly important for pathogenesis. The normal expression profile of the protein as described here may therefore be altered under pathological conditions.

Keywords Agmatine · Calretinin · Polyamines · Habenula · Epithalamus · Depression

Abbreviations

Agm	Agmatinase
Agm-GST	GST fusion protein containing amino acids 176–353 from Agm sequence
Agm-His	6His-tagged thioredoxin fusion protein containing amino acids 176–353 from Agm sequence
Arg I	Arginase I
Arg I-GST	Fusion protein containing amino acids 113–323 from Arg I sequence
BSA	Bovine serum albumin
CA	Ammons horn
DAB	Diamino benzidine
DG	Dentate gyrus
GST	Glutathion-S-Transferase
LHb	Lateral habenula
MD	Mediodorsal thalamus
MHb	Medial habenula
MVe	Medial vestibular nucleus
NGS	Normal goat serum
ODC	Ornithine decarboxylase
Opt	Optical tract
PB	Phosphate buffer
PBS	Phosphate buffered saline
PBS/BSA	PBS with albumine
PrH	Prepositus hypoglossal nucleus
PV	Paraventricular thalamic nucleus

C. Derst · D. Peters · M. Krauss · R. W. Veh · G. Laube (✉)
Center for Anatomy, Institute of Integrative Neuroanatomy, Charité-Universitätsmedizin Berlin, Philippstr. 12, 10115 Berlin, Germany
e-mail: gregor.laube@charite.de

H.-G. Bernstein · C. Stich · B. Bogerts
Department of Psychiatry, Medical Faculty, Otto-von-Guericke-University, Magdeburg, Germany

H. Prüss
Abteilung für Experimentelle Neurologie und Klinik für Neurologie, Charité-Universitätsmedizin Berlin, Berlin, Germany

Py	Pyramidal tract
RT	Room temperature
SON	Supraoptic nucleus
SpdS	Spermidine synthase

Introduction

Polyamines may be synthesized via two distinct pathways, both leading to the formation of the diamine putrescine (Agostinelli et al. 2010; Pegg 1986; Sastre et al. 1996; Satriano 2003). In different two-step reactions, urea and carbon dioxide are removed from the amino acid arginine. The relevant enzymes catalyzing the "classical" pathway are arginase (EC 3.5.3.) and ornithine decarboxylase (EC 4.1.1.17; ODC), while the alternative pathway is driven by arginine decarboxylase (EC 4.1.1.19) and agmatinase (EC 3.5.3.11; Agm), first removing carbon dioxide by arginine decarboxylyase and then urea by agmatinase. So far it is not known, whether the alternative pathway is indeed used to synthesize polyamines. Since the intermediate product agmatine, resulting from the decarboxylation of arginine, is known to act as a putative neurotransmitter or modulator of synaptic transmission (Reis and Regunathan 1998, 2000), it could be assumed that the synthesis and degradation of agmatine rather than polyamine biosynthesis could be the intrinsic purpose of this pathway. Pharmacologically, agmatine, a clonidine displacing substance, acts as an endogenous ligand of imidazoline receptors (Reis et al. 1995) and was measured in different brain regions, especially in the hypothalamus. Apart from being putatively involved in the regulation of blood pressure in the medulla oblongata, several lines of evidence suggest an involvement of agmatine in mental disorders such as schizophrenia and depression (Fiori and Turecki 2008; Halaris and Piletz 2003; Krass et al. 2008; Moinard et al. 2005; Zomkowski et al. 2002). Immunocytochemically, agmatine was localized to neuronal cell bodies in various brain regions (Otake et al. 1998), including cerebral cortex, septum, amygdala, epithalamus, thalamus, and hypothalamus. Given a half life of agmatine in the central nervous system of approximately 12 h (Roberts et al. 2005), the presence of the degrading enzyme agmatinase may serve a crucial regulatory role in agmatine signaling. Agmatinase activity was detected in rat brain subcellular fractions (Sastre et al. 1996) and the highest activity was observed in the hypothalamus, medulla oblongata, and hippocampus, while lower levels were measured in striatum and cerebral cortex. However, even in regions displaying relatively low agmatinase activity an expression in distinct cell types may still be important for local circuitry and also integrative functions. In order to identify the cellular sites of agmatinase expression, and thus also putative regulatory sites controlling agmatine activity, we raised and characterized a rabbit polyclonal antibody against rat agmatinase. Using this antibody, we localized agmatinase to cell bodies and neuropil in selected areas of rat and human brain, including hypothalamus, thalamus, epithalamus, hippocampus, cerebral cortex, and cerebellum.

Materials and methods

Molecular biology and protein chemistry

A 586 bp fragment of rat agmatinase cDNA nucleotides 523–1,109 (GenBank-Acc.No. XM_216570) encoding the C-terminal 179 amino acids of the protein was PCR amplified and cloned into the bacterial expression vectors pGEX-4T-1 [Pharmacia, glutathione-S-transferase (GST) fusion protein] and pET32b(+) [Novagen, 6His-tagged thioredoxin (6His) fusion protein] using *XhoI* restiction sites. Sequence and orientation of the inserted agmatinase cDNA fragment of both vectors were controlled by DNA sequencing. Agmatinase-GST-fusion protein (Agm-GST) and agmatinase-His protein (Agm-His) were over-expressed in the *E. coli* strain BL21DE3 and purified using either Glutathion-Sepharose 4B (GST, Pharmacia Biotech) or Ni^{2+}-NTA agarose (His, Qiagen) as described by the manufacturer. To remove possible cross-reactivities against the closest structural homologue, arginase (see below), similar fusion proteins for arginase I (Arg1-GST, Arg1-His) were constructed (nucleotides 363–1,328 of GenBank Acc.No. NM_017134 encoding the C-terminal 211 amino acids) and purified.

Antibodies

Generation of a monospecific affinity-purified antibody against agmatinase

The generation, purification, and characterization of the monospecific antibody against agmatinase were performed as previously described (Krauss et al. 2006). Briefly, rabbits were immunized with purified Agm-GST fusion protein. The activity of the crude serum was tested against the fusion proteins Agm-GST, Agm-His, Arg1-GST, and Arg1-His. The serum dilution optimal for affinity purification was determined by ELISA. Purification was performed in a three-step procedure. Nitrocellulose membranes were loaded with the cognate antigen Arg-His for removal of potential cross-reactivities for 2 h at room temperature (RT) followed by affinity absorption on

Agm-His-loaded (10 µg/ml in PBS) membranes. Generally, the different membranes were rinsed 3 times in PBS and blocked with 5% normal goat serum for 1 h at RT after loading proteins. For affinity purification, the membranes were incubated with the antiserum diluted 1:1,000 in 5% NGS in PBS overnight at 4°C. After washing, bound antibodies were eluted with 200 mM glycine–HCl, pH 2.5, supplemented with 0.9% NaCl and 0.1% bovine serum albumin for 30 min at RT. Eluted antibodies were subsequently dialyzed against PBS and 20 mM phosphate buffer, pH 6.0, at 4°C. The dialyzed antibody was then loaded on a SP-Sepharose fast flow column at 4°C. Bound antibodies were eluted with 200 mM carbonate buffer, pH 9.0, pooled and then again dialyzed against PBS. The concentrated affinity-purified antibody was aliquoted and stored frozen. Activity was determined with indirect and competitive ELISA assays (Fig. 1).

Preparation of rat tissue

All animal experiments were conducted in accordance with the guidelines of the European Communities Council directive 86/609/EEC and were approved by the Regional Berlin Animals Ethics Committee (LaGeSo No. G 0168/01).

For immunocytochemistry, adult male Wistar rats were deeply anaesthetized using a mixture of Ketavet (Parke-Davis) and Domitor (Pfizer). The animals were then perfused transcardially with 0.9% NaCl solution for 1 min followed by a fixative composed of 4% paraformaldehyde, 0.05% glutaraldehyde, and 0.2% picric acid for 20 min. For immunofluorescence, 4% paraformaldehyde only was used as fixative. Brains were removed from the scull. Tissues were rinsed extensively in 0.1 M phosphate buffer, and freeze-protected with 1 M sucrose in 0.1 M

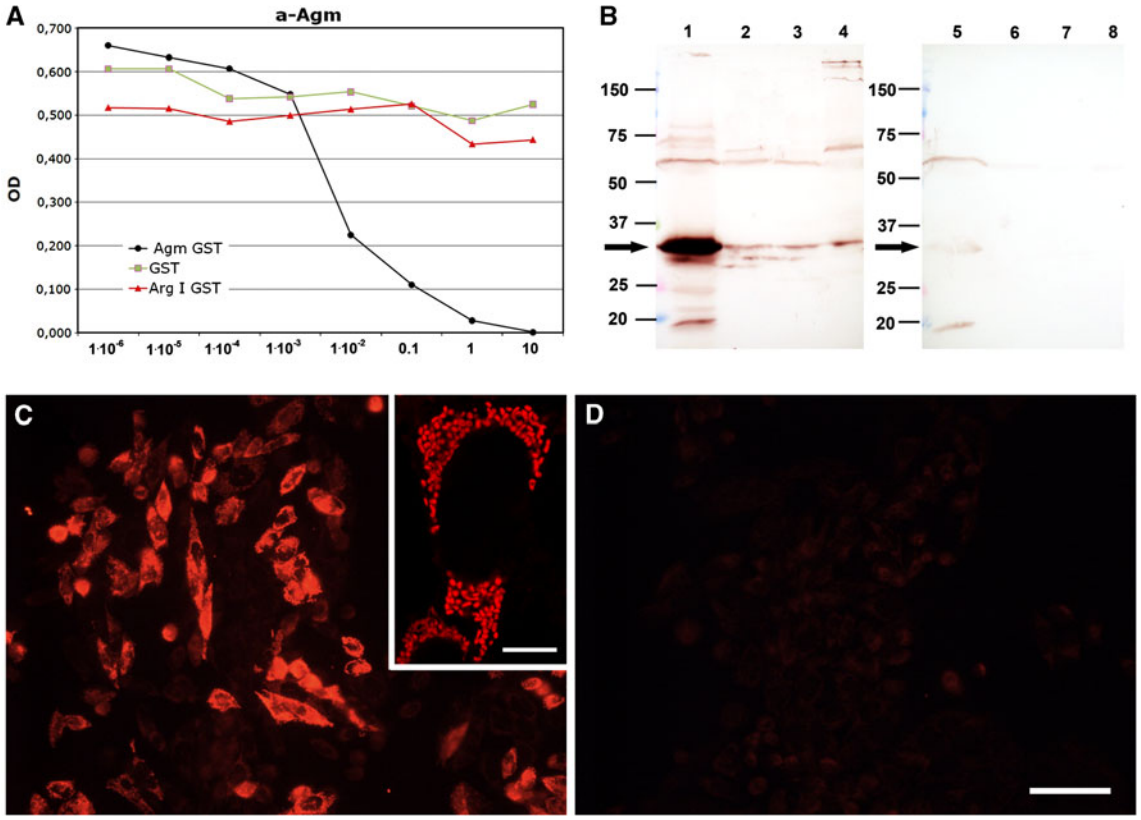

Fig. 1 Characterization of affinity purified anti-agmatinase antibody (a-Agm). **a** In a competitive ELISA assay, the antibody was pre-incubated at a dilution of 1:15,000 with increasing concentrations of either the corresponding antigen used for immunization (Agm-GST) or the distantly related arginase I-GST (Arg I-GST), and GST only. With Agm-GST, 1–10 µg/ml protein completely blocked the activity against Agm-GST at the given dilution. Pre-incubation with arginase I-GST and GST only mildly affected anti-Agm activity. **b** Western blot showing a-Agm activity on blotted homogenates (150 µg protein loaded) from rat liver (*1*, *5*), thalamus (*2*, *6*), cerebellum (*3*, *7*), and cerebral cortex (*4*, *8*). Lanes *1–4* were obtained using a 1:100 dilution of a-Agm. In lanes *5–8*, a-Agm was pre-incubated with 20 µg/ml Agm-GST. The band traveling at approximately 32 kDa, which was robustly expressed in rat liver, was effectively blocked by pre-incubation with the antigen (*arrows*). **c** COS cells transfected with the full length c-DNA for rat Agm displayed intense immunoreactivity when incubated with a-Agm at a dilution of 1:200. At higher magnification (inset in **c**), the immunoreactivity was localized to numerous mitochondria surrounding the immuno-negative nucleus. **d** With non-transfected COS cells, an immunosignal was not detected. *Scale bars* = 50 µm in **c**, **d**; 10 µm in the inset in **c**

phosphate buffer. Tissue was frozen at −60°C in hexane and stored frozen at −80°C until use. For immunocytochemistry, a total of 3 rats and 90 frontal sections were analyzed. Immunocytochemical double labeling experiments were performed 3–5 times for each combination of antigens.

For Western blotting, adult male Wistar rats were anaesthetized with halothane and killed by cervical dislocation. Tissues were rapidly dissected, cut into pieces on a cold metal plate at 0°C, transfered to homogenization buffer supplemented with protease inhibitors (320 mM sucrose, 4 mM HEPES, 1 µg/ml aprotinin, 1 µg/ml pepstatin A, 1 µg/ml leupeptin, 1 µg/ml phenylmethylsulfonylfluoride; pH 7.4) and homogenized with a supersonic homogenizator (Bandelin UW70). The homogenates were centrifuged at 4°C for 10 min at 1,200×g. The supernatants were collected and protein concentration was determined by a bicinchoninic acid assay. 150 µg protein per lane was loaded. A total of four rat brains and livers, separately treated, were used for Western blotting experiments. Specific labeling for Agm (a-Agm 1:100) was reproduced three times and was blocked by pre-incubation with 20 µg/ml Agm-GST (1 h at RT).

Preparation of human tissue

All brains were obtained from pathologists or from medical examination officers, with the full consent of each family and in accordance with the ethics and rules outlined by German law and the local ethics commission of the University of Magdeburg. Brains of four individuals without neurological or psychiatric disorders (two males, 54 and 63 years; two females, 54 and 61 years) were studied.

Brains were removed between 9 and 41 h after death. Tissue preparation was performed as described previously (Bernstein et al. 1999). Briefly, brains were fixed in toto in 8% phosphate-buffered formaldehyde (pH 7.0) for 2 months. After embedding the brains in Paraplast® (McCormick Scientific, St. Louis, MO, USA), serial coronal 20-µm-thick sections were cut on a microtome and mounted on slides. Every 50th section was stained for morphological orientation (combined Cresyl Violet and myelin staining according to Nissl and Heidenhain-Woelcke).

Immunocytochemistry

Immunoperoxidase

Immunoperoxidase labeling was performed using standard DAB/nickel immunoperoxidase protocols as described previously (Krauss et al. 2007). Free-floating sections were treated with 1% sodium-borohydride in PBS for 15 min, washed with phosphate-buffered saline (PBS) and incubated in a solution containing 10% normal goat serum (NGS), 0.3% Triton X-100, and 0.05% phenylhydrazine in PBS for 30 min. Anti-Agm antibody was diluted 1:1,000 and 1:250, respectively, in 10% NGS, 0.3% Triton X-100 supplemented with 0.1% sodium azide and 0.01% thimerosal and incubated for 36 h at 8°C. After washing for 1 h in PBS and another hour in PBS containing 0.2% bovine serum albumin (PBS/BSA), the sections were incubated in biotinylated secondary goat anti-rabbit antibody (Vector, 1:2,000 in PBS/BSA) for 24 h at 8°C. The sections were again washed as described above and further incubated for 6 h with an avidin-biotinyl-peroxidase-complex (Vector Elite ABC kit) in PBS/BSA. After the final washing, bound peroxidase was visualized in a solution containing 1.4 mM DAB, 10 mM imidazole, 6.6 mM nickel ammonium sulfate, and 0.15% H_2O_2 in 50 mM Tris/HCl buffer, pH 7.4. All sections were developed for 15 min. Labeled sections were mounted, dehydrated and cover-slipped with Entellan.

Immunofluorescence

The incubation protocol used for immunofluorescence labeling of rat brain tissue was identical with the immunoperoxidase protocol except for phenylhydrazine which was not used and normal donkey serum instead of NGS which was used as blocking reagent. Secondary antibodies used were goat anti-rabbit CY3, goat anti-mouse CY2, and donkey anti-goat CY2. Labeled sections were mounted on slides, air-dried, dipped in xylene, and cover-slipped with DPX. For double-labeling experiments, commercial antibodies against calretinin (Arai et al. 1996; Winsky et al. 1996) (1:15,000, AB1550, raised in goat; Chemicon, Temecula, CA, USA), parvalbumin (Celio et al. 1988) (1:5,000, P-3171, raised in mouse; Sigma, St Louis, MO, USA), calbindin (Celio et al. 1990) (1:5,000, C-8666, raised in mouse; Sigma), were used.

For controls, either primary or secondary antibodies were omitted. No labeling was detected under these conditions. To further verify the specificity of anti-Agm-labeling, the purified antibody was pre-incubated with the corresponding antigen at concentrations (10, 20 µg/ml) previously determined in a competitive ELISA assay. However, already at 10 µg/ml immunocytochemical labeling of brain sections was completely blocked.

For immunofluorescence labeling of transfected cells, the cells were washed twice with PBS, and fixed in 4% formalin in 0.1 M phosphate buffer, pH 7.4, for 30 min at RT. After three rinses with PBS, they were incubated with blocking solution containing 5% normal goat serum and 2% BSA dissolved in PBS supplemented with 0.1% Triton X-100 for 1 h at RT. Incubation with the primary antibodies diluted in blocking solution was performed at 4°C

overnight. After two rinses with PBS, cells were incubated in the dark with goat anti-rabbit CY3 secondary antibody diluted in 2% bovine serum albumin in PBS supplemented with 0.1% Triton X-100 for 1.5 h at RT. After two rinses with PBS and one rinse in water, coverslips were quickly dehydrated and mounted on glass slides with DPX.

Agmatinase immunocytochemistry on human brain sections

Paraffin sections were collected at intervals of about 1 cm, starting from the level 1 cm rostral to the genu of the corpus callosum down to the level of the inferior olivary nuclei. After dewaxing, the sections were boiled in 10 mM citrate buffer (pH = 6.0) and then pre-incubated with methanol/H_2O_2 to suppress endogenous peroxidases. After repeated washing with phosphate-buffered saline (PBS), the polyclonal antibody was applied at a dilution of 1:400 in PBS. For visualization, the avidin–biotin method (Vectastain-peroxidase kit) with 3,3′-diaminobenzidine as chromogen was used. The color reaction was enhanced by adding 2 ml of a 0.5% nickel ammonium sulfate solution to the diaminobenzidine as described previously (Bernstein et al. 1999). The procedure yielded a dark purplish-blue to dark-blue color reaction product. For negative controls, the primary antibody was replaced with buffer or normal serum.

Western blotting

For sodium dodecyl sulfate polyacrylamide gel electrophoresis, 12% acrylamide gels composed of 0.38 M Tris–HCl, 0.1% SDS, 0.2–0.6% BIS, 0.025% APS, and 0.025% TEMED were used. Tissue homogenates were boiled for 4 min at 96°C, centrifuged, and loaded to the gels at 50 µg protein per lane. Gels were blotted on nitrocellulose. The blots were blocked with 5% milk powder in Tris buffered saline (20 mM Tris–HCl, 150 mM NaCl, pH 7.3) and incubated with anti-Agm antibody at 1:100 overnight at 4°C. Bound antibody was detected with alkaline phosphatase coupled secondary goat anti-rabbit antibody (Vector, AP-1000) at 1:2,000 for 1 h at RT and visualized with 4.6 µM nitro blue tetrazolium, 5 mM magnesium chloride, 26 µM 5-bromo-chloroindolyl-phosphate *p*-toluidine salt, and 100 mM sodium chloride in 50 mM Tris–HCl, pH 9.5.

Heterologous expression of Agm in COS cells

COS-1 cells were cultured at 5% CO_2 in RPMI 1640 medium (Sigma–Aldrich) with 10% fetal calf-serum on 24-well plates containing glass cover slips. Cells were transiently transfected using jetPEI (Polyplus-transfection, Illkirch, France) according to the manufacturer's instruction with 1 µl of jetPEI and 0.5 µg of plasmid DNA containing full length Agm cDNA cloned into the expression vector pcDNA3.1. 48–72 h after transfection, cells were washed in PBS followed by fixation in 4% phosphate-buffered formaldehyde and washing in PBS.

Results

Agm, a member of the arginase family, shares a maximum of 38% sequence identity in a 55 amino acid overlap and 17% total identity with rat arginase I (Arg I), the most closely related member of this family. For immunization, the carboxy-terminal half (amino acids 176–353) of the protein was chosen and expressed as bacterial fusion protein. During purification, the anti-Agm raw serum was pre-absorbed with Arg I fusion protein in order to remove potential cross-reactivities. The affinity-purified antibody was then characterized in a competitive ELISA assay (Fig. 1a). With increasing concentrations of Agm-GST fusion protein, but not with GST only and Arg I-GST, the activity of the anti-Agm antibody (1:15,000) was competitively decreased and finally completely blocked at 10 µg/ml. We thus concluded to the mono-specificity of the anti-Agm antibody and further characterized it by Western blotting using rat liver and brain homogenates (Fig. 1b). Very strong immunoreactivity was observed with a prominent band traveling at approximately 32 kDa in rat liver, 6 kDa below the molecular weight of the rat Agm non-processed translation product. Computational analysis of the non-processed sequence (MitoProt II-v1.101) revealed a potential cleavage site at residue 40 and a probability of mitochondrial export of 0.944 (Claros and Vincens 1996). The calculated molecular weight of the putative 40 amino acid targeting sequence is 4.2 kDa, thus the processed sequence would closely match the band detected in rat liver. The same protein was detected in several rat brain areas, including thalamus, cerebral cortex, and cerebellum. However, the amount of protein in brain homogenates was significantly less when compared to liver homogenate. In order to test for the specificity of the antibody reaction, pre-incubation with the fusion protein used for immunization was performed (Fig. 1b, right column). Despite the strong expression, the band at 32 kDa was almost completely blocked in rat liver and completely absent in brain fractions. By contrast, minor bands detected at 20 and 60 kDa in liver homogenate persisted and were concluded to reflect non-specific interaction. The biochemically characterized antibody was then tested with immunocytochemistry on transfected COS cells expressing full length rat Agm (Fig. 1c). In these cells, a strong Agm expression was detected after transfection, while in non-transfected COS

cells, no immunoreactivity was detected (Fig. 1d), thus demonstrating the ability of the affinity-purified antibody to immunocytochemically detect Agm. Furthermore, the subcellular distribution of the Agm signal strongly supported a mitochondrial targeting of the protein (Fig. 1c, inset), which so far was only theoretically predicted.

Regional and cellular distribution of Agm immunoreactivity in rat brain

Given that the anti-Agm antibody specifically interacted with its target protein in aldehyde-fixed cells, we then tested it on rat brain sections in order to identify potential regional sources of agmatine degradation. Generally, Agm-like immunoreactivity was most obviously detected in neurons, but also to some extent in neuropil areas (compare different dilutions in Fig. 2a, d). This labeling of brain tissue could be completely abolished by pre-incubating the antibody with the respective antigen (not shown) and was thus considered specific.

In rat cerebral cortex (Fig. 2a–c), strongly labeled interneurons occured in all layers but were most frequently observed in layers II/III (Fig. 2b, c, e, f) and only rarely found in layers V/VI. Cell bodies and processes of these cells were both labeled. On some occasions, the processes were displayed in great detail allowing to follow the dendrites along a length of more than 200 μm (Fig. 2c). The overall distribution of these strongly immunopositive interneurons was very similar to that observed for the calcium binding protein calretinin (Jacobowitz and Winsky 1991). Compared to these interneurons, labeling in cortical granule cells (Fig. 2e) and pyramidal neurons (Fig. 2f) was considerably weaker, though clearly detectable under conditions of increased antibody concentration (Fig. 2a–c). Also, the neuropil of layers I–III was more intensely labeled than in the other layers.

In the hippocampal formation, similar as in the neocortex, interneurons were most prominently labeled (Fig. 2g, h). In the CA area, the somata of these interneurons were mostly localized in the pyramidal cell layer, but also observed in stratum radiatum and stratum oriens. In the dentate gyrus, the majority of strongly labeled interneurons were observed in a subgranular position (Fig. 2i, j). In order to characterize the Agm-positive subpopulation of hippocampal interneurons, immunofluorescence double labeling for the calcium-binding proteins calretinin, parvalbumin, and calbindin was performed (Fig 3). A co-localization was observed with calretinin (Fig. 3a, b) only, while parvalbumin (Fig. 3c, d) and calbindin (Fig. 3e, f) containing neurons clearly constituted different populations not displaying any Agm-like immunoreactivity. A co-localization with calretinin was also observed in other brain areas known to prominently express calretinin, like the cerebral cortex, and the triangular septum (not shown). Similar to the cerebral cortex, labeling was generally weaker in hippocampal pyramidal neurons than in interneurons, but still clearly detectable when using increased antibody concentrations (compare Fig. 2 G/H hippocampus, A/D cortex).

In the cerebellar cortex, by contrast, projection neurons most prominently expressed Agm-like immunoreactivity, displaying Purkinje cell bodies as well as their dendritic trees (Fig. 4a, b). In the molecular layer, in addition to Purkinje cell dendrites, the neuropil was diffusely labeled while interneurons were not observed in this area. By comparison, the granule cell layer was only weakly labeled, except for locally occurring interneurons clearly displaying the morphological characteristics of unipolar brush cells (Fig. 4b, inset). The somata and dendritic arbors of these neurons were both strongly labeled. With immunofluorescence double labeling (Fig. 4c, d), these cells were identified as belonging to the calretinin expressing subset of unipolar brush cells (Floris et al. 1994).

In the diencephalon, Agm-like immunoreactivity was highly contrasting displaying strong labeling in epithalamic areas while the majority of thalamic nuclei were largely unlabeled (Fig. 5a). In the epithalamus, strong labeling of neuronal cell bodies and, to a lesser extent, neuropil was observed in the medial habenula. Here, immunopositive neurons were restricted to lateral parts of the medial habenula, most notably a dorsolateral group of small and densely packed neurons (Fig. 5b), directly adjacent to the lateral habenula. By contrast, the neuropil was most intensely labeled at the medial border of the medial habenula, just beneath the ependyma. Very robust neuronal labeling was also detected in dorsal midline thalamic areas, especially the paraventricular thalamic nucleus (Fig. 5a, c). Here, strongly labeled cell bodies were observed in the lateral parts of the nucleus outlining the adjacent mediodorsal thalamic nucleus with some neurons infiltrating this area. Neuropil labeling, though less intense, was also clearly present in the dorsal midline thalamic area. Otherwise, most thalamic areas were largely devoid of any neuropil immunoreactivity. By contrast, in the hypothalamus a moderate neuropil labeling was generally present, thus demarcating the thalamic-hypothalamic border. Scattered immunoreactive neurons frequently displaying several processes were observed in many hypothalamic areas. In the supraoptic nucleus, labeling of neurons was comparatively less intense but also inhomogeneous ranging from moderately to weakly labeled somata (Fig. 5d, e).

In the brain stem (Fig. 5f), immunoreactivity was again most prominent in neurons, e.g. in the reticular formation and the inferior olive (Fig. 5g). By contrast, the medial vestibular nucleus (Fig. 5f) displayed robust Agm-like immunoreactivity in the neuropil.

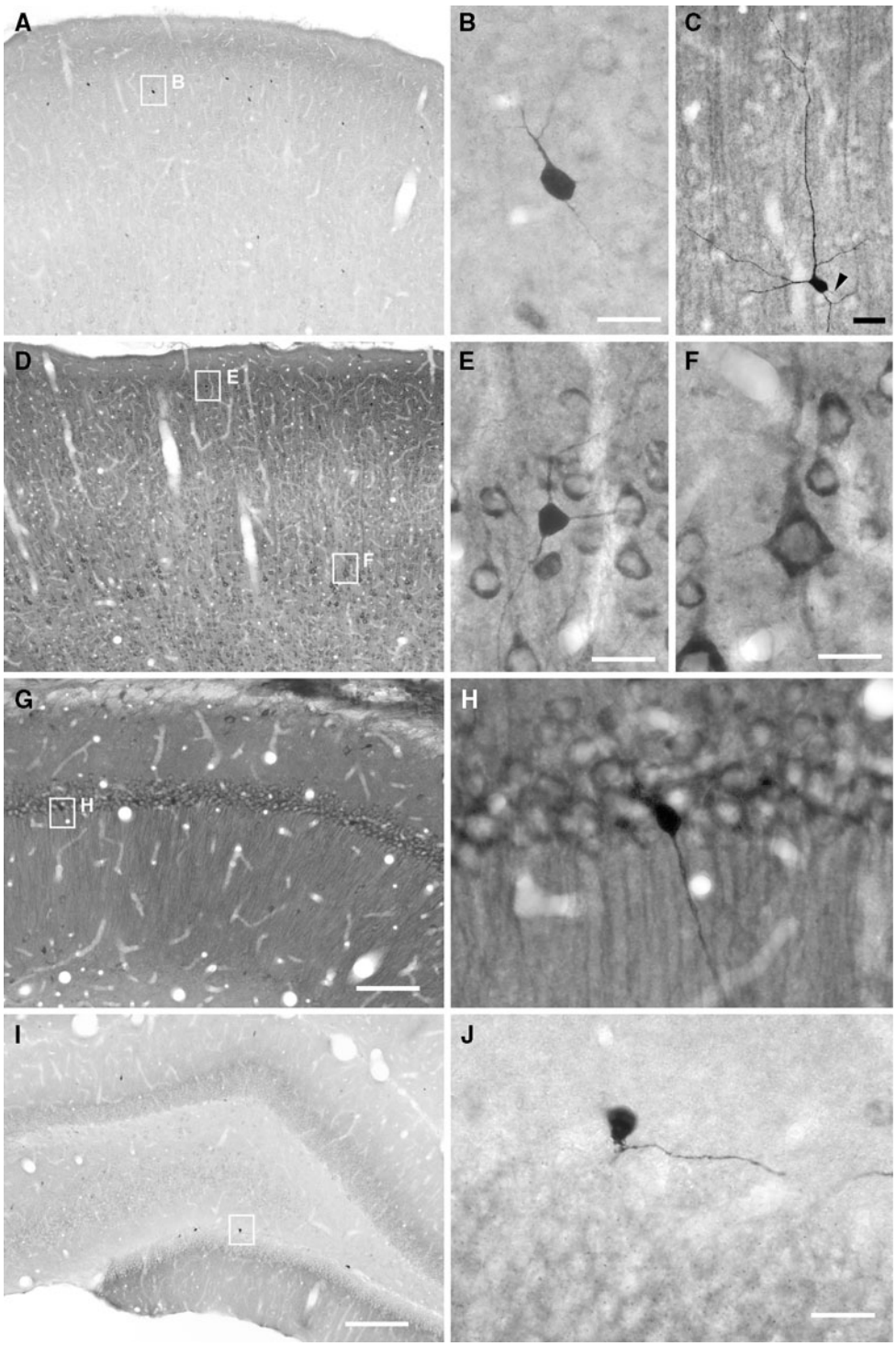

Fig. 2 Agm in cortical neurons. Two dilutions (1:1,000 in **a–c** and **i–j**; 1:250 in **d–h**) of the a-Agm antibody were used in order to differentiate between most strongly labeled interneurons (**a–c**, **i–j**) and moderately immunopositive principal neurons of cerebral cortex (**d–f**) and hippocampal formation (**g–h**). In the cerebral cortex (**a–f**), strongly labeled interneurons were most numerous in cortical layers II/III (**a**). Dendritic and axonal (*arrowhead* in **c**) processes of these neurons (**b**, **c**) were frequently observed and could partly be followed over relatively long distances (**c**). By contrast, granule (**e**) and pyramidal (**f**) neurons were less intensely but clearly labeled. In the hippocampal CA1 area (**g**, **h**), immunoreactive interneurons were frequently associated with the pyramidal cell layer (**h**). In pyramidal neurons, immunoreactivity was observed in somata as well as dendrites crossing stratum radiatum and lacunosum-moleculare. In the dentate gyrus (**i**, **j**), immunoreactive interneurons were frequently observed in a subgranular position. The *boxed areas* in **a**, **d**, **g**, **i** are shown at higher magnification in the *right panel*. *Scale bars* represent 100 μm in **a**, **d**, **g**; 200 μm in **i**; 25 μm in **c**, and 20 μm in **b**, **e**, **f**, **h**, **j**

Regional and cellular distribution of Agm immunoreactivity in human brain

In human forebrain, cerebellum, and brain stem, Agm-like immunoreactivity was widely spread but not homogeneously distributed. There were no apparent gender differences in the regional and cellular localization of the protein. To determine whether postmortem time may affect immunocytochemical labeling, brains were processed after different postmortem delays. There were no obvious differences detected with regard to intracellular labeling intensity and/or regional labeling patterns when comparing sections from brains with short-term (9 h) versus long-term (41 h) postmortem intervals.

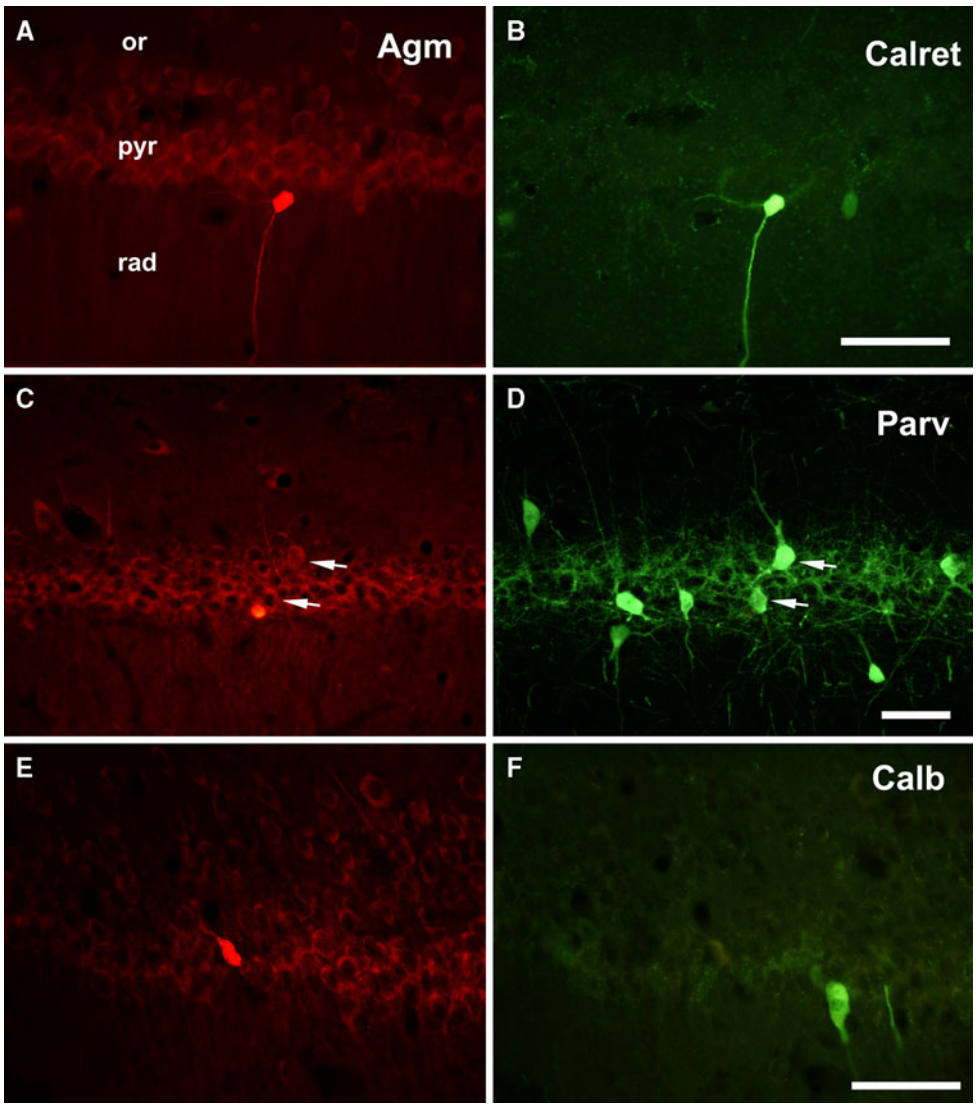

Fig. 3 Immunofluorescence double labeling for Agm (*left panel*, **a**,**c**,**e**; CY3) and calcium binding proteins (*right panel*; CY2) and calcium binding proteins calretinin (**b**), parvalbumin (**d**), and calbindin (**f**) in the hippocampal CA1 area. A co-localization was observed with calretinin only (**a**, **b**) while in parvalbumin (**d**) and calbindin (**f**) cells Agm-like immunoreactivity (**c**, **e**) was never detected (the *arrows* in **c**, **d** label parvalbumin cells in the proximity of the Agm cell shown in **c**). All hippocampal interneurons expressing Agm did also contain calretinin. A complete identity of Agm and calretinin containing interneurons was also observed in the cerebral cortex (not shown). Note the moderate Agm immunoreactivity in pyramidal neurons (**a**, **c**, **e**). *or* Stratum oriens, *pyr* stratum pyramidale, *rad* stratum radiatum. *Scale bars* represent 50 μm

On the cellular level, Agm-immunoreactivity was mainly confined to several types of neurons, predominantly interneurons. Besides, moderately labeled white matter parafascicular oligodendrocytes and occasionally astrocytes belonging to the membrana limitans gliae were observed.

In the cerebral cortex (Fig. 6a), thirteen different palaeo- and neocortical areas were studied: gyrus semilunaris, gyrus parahippocampalis, gyrus entorhinalis, gyri temporales inferior and medius, gyri longus and breves insulae, gyrus precentralis, gyrus postcentralis, gyri frontales medius and superior, and gyrus cinguli. In all these cortical areas, similar patterns of Agm-immunoreactive neurons were observed. Frequently, layer II and IV interneurons displayed an intense immunolabeling. Some pyramidal cells were also observed to express the protein. In the entorhinal cortex, Agm immunoreactivity was localized in neurons forming the pre-α clusters and also in interneurons. Intracellularly, the immunoreaction was detected in neuronal perikarya and dendrites. Typically, cell nuclei did not contain any reaction product. Occasionally, the neuropil showed a moderate immunolabeling.

In the hippocampus (Fig. 6b), numerous interneurons and dentate gyrus granule neurons displayed strong to moderate immunolabeling. Occasionally, weakly labeled hippocampal pyramidal cells were observed. However, pyramidal neurons were frequently surrounded by immunoreactive punctae, presumably representing axon terminals.

The hypothalamus was clearly among the brain regions most prominently expressing Agm. The protein was detected in neurons of several hypothalamic nuclei. The most pronounced immunolabeling was observed in the paraventricular and especially in the supraoptic nucleus (Fig. 6c), but also in the lateral hypothalamic, the suprachiasmatic and the arcuate nucleus. Some immunopositive

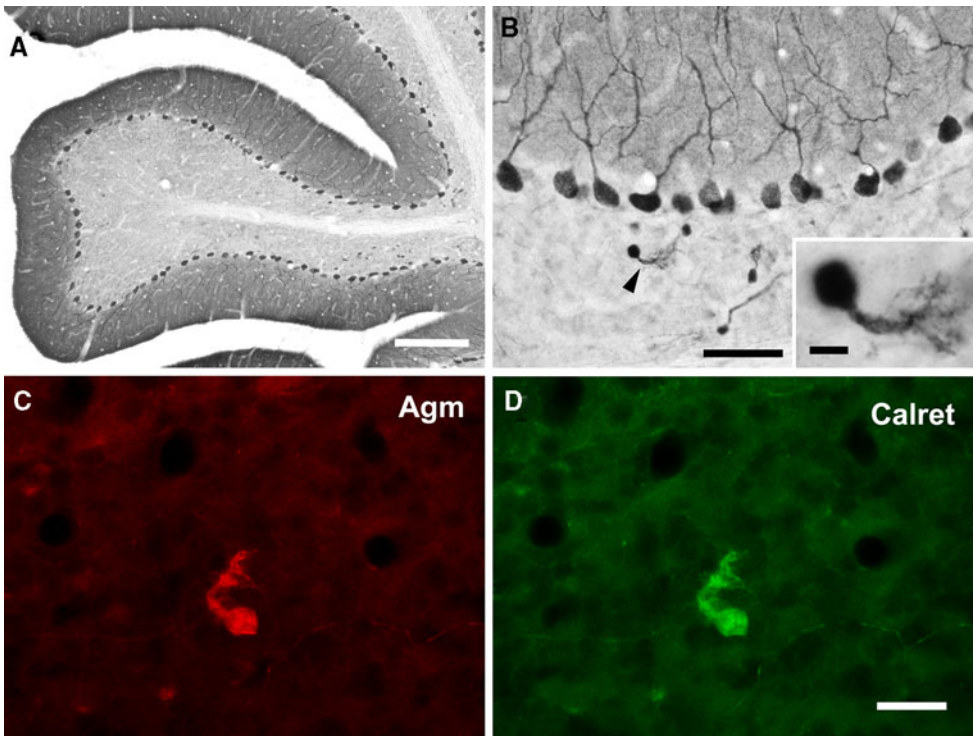

Fig. 4 Agm-immunoreactivity in the cerebellar vermis. Purkinje cell somata and dendritic trees were intensely labeled throughout folia (**a**, **b**). In addition, a diffuse labeling of the neuropil was observed in the molecular layer. The only other distinctly labeled cell type displayed the morphological characteristics of locally occurring unipolar brush cells (*arrowhead* in **b** and *inset*) located in the granule cell layer (**b**). With double labeling immunofluorescence (**c**, **d**), immunopositive cells were shown to belong to the calretinin-containing group of unipolar brush cells. *Scale bars* represent 200 μm in **a**, 50 μm in **b**, 10 μm in *inset*, 20 μm in **c**, **d**

neurons were detected in the intercalate nucleus facing the mammillary bodies.

Within the thalamus, several nuclei including the ventroposterior medial thalamic nucleus, the anterodorsal and the mediodorsal nuclei prominently expressed Agm-like immunoreactivity. In the lateral and medial geniculate nuclei, almost all neurons were immunolabeled for Agm. In particular, in the epithalamic habenular complex (Fig. 6d) a densely labeled network of Agm-immunoreactive fibers embracing numerous small Agm-expressing neurons was evident.

In the cerebellum, somata of most Purkinje neurons were intensely Agm-immunopositive (Fig. 6e). Occasionally, the reaction product was also observed in Purkinje cell dendrites. In addition, Agm-immunolabelling was detected in a subpopulation of neurons of deep cerebellar nuclei (i.e. dentate and globose nuclei).

Robust immunolabeling for Agm was observed in some brain stem nuclei, especially in neurons of the trigeminal and vestibular nuclei as well as in the inferior olivary nucleus (Fig. 6f).

Further areas displaying noticeable Agm-labeling were observed in the forebrain (strongly immunoreactive neuropil in the caudate nucleus; scattered intensely labeled neurons in the accumbens nucleus; moderately labeled neurons in the septal region and in the diagonal band of Broca) and midbrain (strongly immunopositive neurons in the ventral tegmentum, the parabrachial nucleus and the substantia nigra pars reticularis and pars compacta).

Discussion

Since the initial observation that the guanidino group bearing diamine agmatine is identical with clonidine-displacing substance and thus may act as an endogenous ligand at imidazoline receptors in the brain (Li et al. 1994), several lines of evidence have suggested that agmatine may serve a role as a neurotransmitter (Reis and Regunathan 1998; Reis et al. 1998) or neuromodulator (Galea et al. 1996; Olmos et al. 1999; Halaris and Plietz 2007). However, although controversially discussed with respect to endogenous formation (Coleman et al. 2004; Iyo et al. 2006), agmatine may also serve as a precursor in polyamine synthesis, since its degradation by the action of Agm results in the formation of the diamine putrescine. In both scenarios, the local expression of Agm is required in order to either inactivate the neurotransmitter/neuromodulator or provide the substrate for spermidine/spermine synthesis. In either case, a detailed analysis of local brain Agm expression may help to elucidate potential functional roles for agmatine in brain circuitry. According to our data, Agm is most prominently expressed in neurons, although with increasing antibody concentration oligodendrocytes were also visualized (compare Fig. 5d, e). The highest levels of Agm-like immunoreactivity were clearly confined to neocortical and hippocampal interneurons, co-expressing the calcium-binding protein calretinin. Besides these scattered interneurons, distinct nuclei like the thalamic paraventricular nucleus, or distinct principal neurons like cerebellar

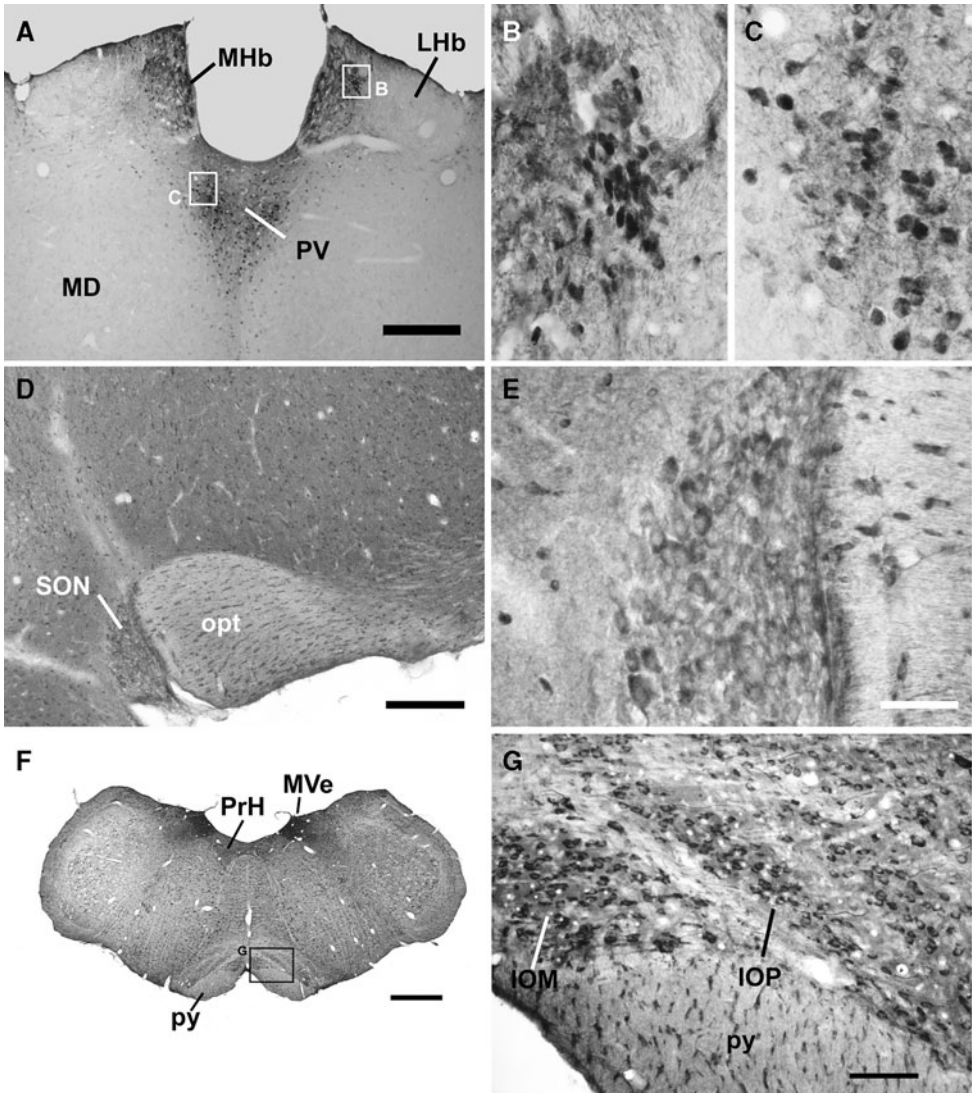

Fig. 5 Agm-like immunoreactivity in the diencephalon (**a**–**e**) and brain stem (**f**, **g**). Robust labeling in the epithalamus (**a**–**c**) contrasted with large parts of the thalamus being devoid of any immunosignal, e.g. the mediodorsal thalamus (*MD*). In the epithalamus, the medial habenula (*MHb*; **a**, **b**) and the paraventricular thalamic nucleus (*PV*; **a**, **c**) contained intensely labeled neurons (**b**, **c**) embedded in immunoreactive neuropil. By contrast, the lateral habenula was clearly less immunoreactive with scattered moderately labeled neurons and neuropil in the medial division (not shown) while the lateral division was largely immunonegative. In the hypothalamus (**d**, **e**), generally neuropil was clearly immunoreactive, in contrast to adjacent thalamic areas. Scattered Agm-positive neurons were commonly observed throughout the hypothalamus. In the supraoptic nucleus (*SON*), a subpopulation of magnocellular neurons was more intensely labeled than other neurons in this area (**e**). In the brain stem (**f**, **g**) besides scattered large and prominently labeled neurons, e.g. in the gigantocellular reticular nucleus, the different subnuclei of the inferior olive were also clearly labeled (**g**). The nuclei lining the floor of the 4th ventricle, the prepositus hypoglossal nucleus (*PrH*) and especially the medial vestibular nucleus (*MVe*), additionally displayed dense neuropil labeling. *opt* Optical tract, *py* pyramidal tract, *IOM* inferior olive, medial nucleus, *IOP* inferior olive, principal nucleus. *Scale bars* represent 200 μm in **a**, **d**, **g**; 50 μm in **b**, **c**, **e**; 1 mm in **f**

Purkinje cells, displayed robustly labeled neuronal cell bodies. By comparison, neocortical and hippocampal pyramidal neurons were only weakly labeled under these conditions and required an increased antibody concentration to be clearly visualized (compare Fig. 2a, d). Under these conditions, also neuropil labeling, most notably in cortical and hypothalamic areas, was evident. With respect to rat and human brain as studied here, the immunocytochemical results were mostly very similar indicating a similar distribution and therefore possibly similar functional roles for Agm in these species. Immunocytochemical data showing the distribution of the Agm substrate agmatine exist (Gorbatyuk et al. 2001; Otake et al. 1998; Reis et al. 1998). Accordingly, agmatine-like immunoreactivity was mainly detected in cell bodies. In the neocortex, scattered neurons mostly residing in layers

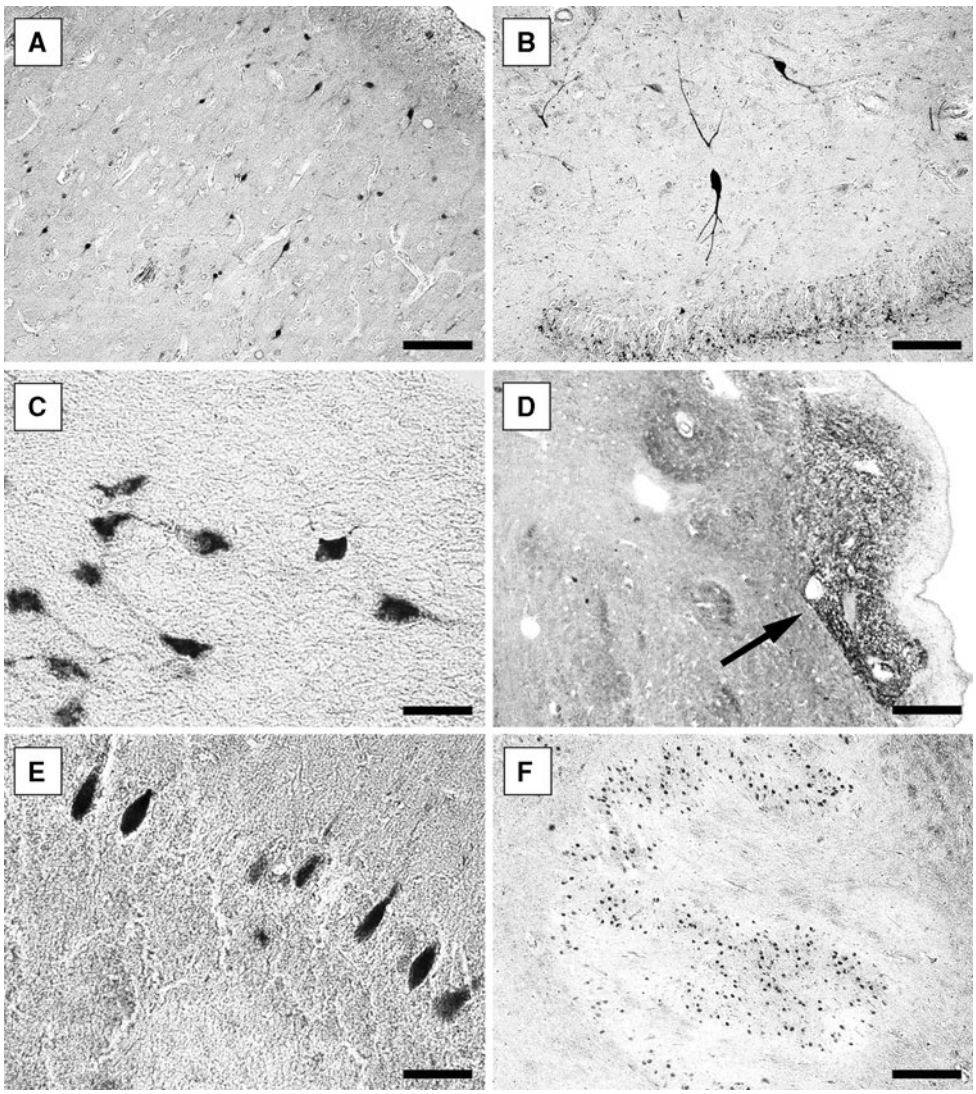

Fig. 6 Agm-like immunoreactivity in human frontal brain sections. In different cortical areas including the temporal cortex (**a**), numerous Agm-positive interneurons were observed, especially in layers II and IV. Immunoreactive pyramidal neurons were also observed. In the hippocampal formation, intensely labeled interneurons were frequently present, as demonstrated in the CA2 area (**b**). By contrast, pyramidal neurons were only weakly labeled. In the hypothalamus, Agm-like immunoreactivity was widely spread and especially prominent in the supraoptic nucleus (**c**). In the epithalamus (**d**), intensely labeled neuropil and small immunoreactive neurons were evident in the habenula (*arrow*). Labeling was observed in the medial and lateral habenula, which were not clearly delineated. Immunoreactivity was also present in several thalamic areas. In the cerebellum, Purkinje cell somata were robustly labeled (**e**). Occasionally, also Purkinje cell dendrites were visualized. In the brain stem, inferior olive (**f**) neurons were prominently labeled. *Scale bars* represent 140 μm in **a**, **f**; 80 μm in **b**; 50 μm in **c**, **e**; 250 μm in **d**

V/VI were observed. By comparison, the majority of Agm-positive interneurons were localized to layers I–IV and also the neuropil of layer I (II/III) was more intensely labeled. Thus, in the cerebral cortex, agmatine and Agm show a largely non-overlapping distribution with respect to immunopositive interneuron somata. By contrast, in the thalamus striking similarities are apparent when comparing the midline nuclei, especially the paraventricular thalamic nucleus (PV), and the majority of the large mediodorsal and lateral thalamic nuclei. Both, agmatine and Agm-containing neurons are highly enriched in the PV and were both not detected in large parts of the thalamus including the mediodorsal and lateral nuclei. Phylogenetically, the PV, being involved with viscero-limbic functions, is considered to be part of the epithalamus (Van der Werf et al. 2002). Interestingly, in the epithalamus also the habenula was immunopositive for agmatine and Agm (compare Fig. 5a), though concentrated in different areas, the lateral and medial habenula, respectively. In the hippocampus, agmatine was detected in CA1 Schaffer collateral terminals (Reis et al. 1998) while Agm is expressed in CA1 pyramidal cells (compare Fig. 2g, h), postsynaptic to these terminals. In the hypothalamus, numerous agmatine-containing cell bodies including neurosecretory neurons of the SON were reported (Gorbatyuk et al. 2001; Otake et al. 1998). Correspondingly, this area also contains scattered Agm-positive cell bodies, immunopositive neurosecretory SON neurons, and labeled neuropil. Taken together, the available data for agmatine and Agm distribution strongly suggest a correlation between the two immunocytochemical profiles, thus mutually corroborating the individual immunocytochemical labeling results. However, it also seems likely that agmatine may serve different cellular functions and may accordingly be locally inactivated. Such a scenario could be involved with agmatine being released from vesicles (e.g. in the hippocampus). Here, Agm would

be expressed in the postsynaptic target cell. In other cases, like SON neurosecretory neurons, agmatine may serve intracellular functions as implied by the localization at endoplasmic membranes near the nuclear envelope (Gorbatyuk et al. 2001) and the converting enzyme Agm being localized in the same type of neuron.

With respect to the second putative function of agmatine/Agm, namely providing an alternative pathway for polyamine synthesis, insight could be expected from the subtractive analysis of available data for ODC and the comparison with spermidine synthase (SpdS) expression (Bernstein and Muller 1999; Krauss et al. 2006; Krauss et al. 2007). Although ODC is highly inducible and thus may be underrepresented with immunocytochemical analysis, it is obvious that at least in some major neuronal populations such as cortical granule neurons and pyramidal cells, hippocampal pyramidal cells, cerebellar Purkinje cells, and, less precisely specified, in the hypothalamus (Cintra et al. 1987), Agm and ODC are both expressed, though no co-localization data are so far available. In these cell populations, SpdS was also detected at weak to moderate levels, except for the hypothalamus which contained many strongly labeled neurons, also present in the SON. Thus, in these neurons it seems unlikely that agmatine synthesis serves as an alternative pathway for putrescine and hence polyamine synthesis.

Using biochemical methods, it was demonstrated that not only agmatinase is enriched in subcellular fractions containing mitochondrial matrix proteins (Sastre et al. 1996), but also that agmatine is transported into rat brain mitochondria (Battaglia et al. 2010a). In accordance with these data, in the present study full length recombinant Agm protein expressed in COS cells was exclusively targeted to mitochondria. With immunocytochemistry on rat brain sections, however, labeling was observed throughout the cytoplasm and thus did not indicate an exclusive localization to mitochondria. Functionally, it was shown that agmatine prevents the Ca^{2+}-dependent induction of permeability transition in rat brain mitochondria (Battaglia et al. 2010b). Agmatine and Agm may therefore be involved in neurodegenerative disorders exhibiting mitochondrial dysfunction (Morais and De Strooper 2010) and indeed agmatine was shown to be effective as an anti-apoptotic agent (Hong et al. 2009). In this context, an increase or decrease in Agm expression could either impair or ameliorate a neuroprotective effect of agmatine. Furthermore, agmatine can affect both the generation of NO (Satriano 2004) as well as the intracellular concentrations of polyamines (Satriano et al. 1998; Vargiu et al. 1999). Interestingly, in regions vulnerable to neurodegeneration like the substantia nigra compacta and the striatum, Agm (not shown) and the polyamine biosynthetic enzyme SpdS (Krauss et al. 2006) were similarly detected in distinct cell populations. Additional studies monitoring the expression of both systems under pathological conditions are clearly required and may shed new light on the underlying mechanisms.

Systemically both, the polyamine and the agmatine system have been discussed in the functional context of psychiatric diseases, notably in depression and schizophrenia (Chen et al. 2010; Fiori and Turecki 2008; Halaris and Piletz 2003; Halaris and Plietz 2007; Krass et al. 2008; Zomkowski et al. 2002). Since agmatine and Agm are prominently expressed in rat brain areas involved with stress regulation, such as the hypothalamus and epithalamus, and given that in the human brain Agm is detected with a very similar pattern, it seems reasonable, based on the available immunocytochemical studies, to hypothesize a possible involvement of the agmatine system and hence Agm under pathological conditions. With this respect, we are currently investigating human brain material from mentally diseased patients in order to verify changes in the expression of Agm possibly reflecting the course of the disease.

Taken together, Agm is prominently but also highly differentially expressed in rat and human brain and may presumably be used as a marker in order to monitor changes in brain neurochemistry possibly causally involved with mental disorders.

Acknowledgments The authors would like to thank Berit Soehl-Kielczinski and Semanur Ünsal for excellent technical assistance.

Conflict of interest statement The authors declare that they have no conflict of interest.

References

Agostinelli E, Marques MP, Calheiros R, Gil FP, Tempera G, Viceconte N, Battaglia V, Grancara S, Toninello A (2010) Polyamines: fundamental characters in chemistry and biology. Amino Acids 38(2):393–403

Arai R, Jacobowitz DM, Nagatsu I (1996) Calretinin is differentially localized in magnocellular oxytocin neurons of the rat hypothalamus. A double-labeling immunofluorescence study. Brain Res 735(1):154–158

Battaglia V, Grancara S, Mancon M, Cravanzola C, Colombatto S, Grillo MA, Tempera G, Agostinelli E, Toninello A (2010a) Agmatine transport in brain mitochondria: a different mechanism from that in liver mitochondria. Amino Acids 38(2):423–430

Battaglia V, Grancara S, Satriano J, Saccoccio S, Agostinelli E, Toninello A (2010b) Agmatine prevents the Ca(2 +)-dependent induction of permeability transition in rat brain mitochondria. Amino Acids 38(2):431–437

Bernstein HG, Muller M (1999) The cellular localization of the l-ornithine decarboxylase/polyamine system in normal and diseased central nervous systems. Prog Neurobiol 57(5):485–505

Bernstein HG, Baumann B, Danos P, Diekmann S, Bogerts B, Gundelfinger ED, Braunewell KH (1999) Regional and cellular distribution of neural visinin-like protein immunoreactivities (vilip-1 and vilip-3) in human brain. J Neurocytol 28(8):655–662

Celio MR, Baier W, Scharer L, de Viragh PA, Gerday C (1988) Monoclonal antibodies directed against the calcium binding protein parvalbumin. Cell Calcium 9(2):81–86

Celio MR, Baier W, Scharer L, Gregersen HJ, de Viragh PA, Norman AW (1990) Monoclonal antibodies directed against the calcium binding protein calbindin d-28k. Cell Calcium 11(9):599–602

Chen GG, Fiori LM, Moquin L, Gratton A, Mamer O, Mechawar N, Turecki G (2010) Evidence of altered polyamine concentrations in cerebral cortex of suicide completers. Neuropsychopharmacology 35(7):1477–1484

Cintra A, Fuxe K, Agnati LF, Persson L, Harfstrand A, Zoli M, Eneroth P, Zini I (1987) Evidence for the existence of ornithine decarboxylase-immunoreactive neurons in the rat brain. Neurosci Lett 76(3):269–274

Claros MG, Vincens P (1996) Computational method to predict mitochondrially imported proteins and their targeting sequences. Eur J Biochem 241(3):779–786

Coleman CS, Hu G, Pegg AE (2004) Putrescine biosynthesis in mammalian tissues. Biochem J 379(Pt 3):849–855

Fiori LM, Turecki G (2008) Implication of the polyamine system in mental disorders. J Psychiatry Neurosci 33(2):102–110

Floris A, Dino M, Jacobowitz DM, Mugnaini E (1994) The unipolar brush cells of the rat cerebellar cortex and cochlear nucleus are calretinin-positive: a study by light and electron microscopic immunocytochemistry. Anat Embryol (Berl) 189(6):495–520

Galea E, Regunathan S, Eliopoulos V, Feinstein DL, Reis DJ (1996) Inhibition of mammalian nitric oxide synthases by agmatine, an endogenous polyamine formed by decarboxylation of arginine. Biochem J 316(Pt 1):247–249

Gorbatyuk OS, Milner TA, Wang G, Regunathan S, Reis DJ (2001) Localization of agmatine in vasopressin and oxytocin neurons of the rat hypothalamic paraventricular and supraoptic nuclei. Exp Neurol 171(2):235–245

Halaris A, Piletz JE (2003) Relevance of imidazoline receptors and agmatine to psychiatry: A decade of progress. Ann N Y Acad Sci 1009:1–20

Halaris A, Plietz J (2007) Agmatine: metabolic pathway and spectrum of activity in brain. CNS Drugs 21(11):885–900

Hong S, Kim CY, Lee JE, Seong GJ (2009) Agmatine protects cultured retinal ganglion cells from tumor necrosis factor-alpha-induced apoptosis. Life Sci 84(1–2):28–32

Iyo AH, Zhu MY, Ordway GA, Regunathan S (2006) Expression of arginine decarboxylase in brain regions and neuronal cells. J Neurochem 96(4):1042–1050

Jacobowitz DM, Winsky L (1991) Immunocytochemical localization of calretinin in the forebrain of the rat. J Comp Neurol 304(2):198–218

Krass M, Wegener G, Vasar E, Volke V (2008) Antidepressant-like effect of agmatine is not mediated by serotonin. Behav Brain Res 188(2):324–328

Krauss M, Langnaese K, Richter K, Brunk I, Wieske M, Ahnert-Hilger G, Veh RW, Laube G (2006) Spermidine synthase is prominently expressed in the striatal patch compartment and in putative interneurons of the matrix compartment. J Neurochem 97(1):174–189

Krauss M, Weiss T, Langnaese K, Richter K, Kowski A, Veh RW, Laube G (2007) Cellular and subcellular rat brain spermidine synthase expression patterns suggest region-specific roles for polyamines, including cerebellar pre-synaptic function. J Neurochem 103(2):679–693

Li G, Regunathan S, Barrow CJ, Eshraghi J, Cooper R, Reis DJ (1994) Agmatine: an endogenous clonidine-displacing substance in the brain. Science 263(5149):966–969

Moinard C, Cynober L, de Bandt JP (2005) Polyamines: metabolism and implications in human diseases. Clin Nutr 24(2):184–197

Morais VA, De Strooper B (2010) Mitochondria dysfunction and neurodegenerative disorders: cause or consequence. J Alzheimers Dis 20(Suppl 2):255–263

Olmos G, DeGregorio-Rocasolano N, Paz Regalado M, Gasull T, Assumpcio Boronat M, Trullas R, Villarroel A, Lerma J, Garcia-Sevilla JA (1999) Protection by imidazol(ine) drugs and agmatine of glutamate-induced neurotoxicity in cultured cerebellar granule cells through blockade of NMDA receptor. Br J Pharmacol 127(6):1317–1326

Otake K, Ruggiero DA, Regunathan S, Wang H, Milner TA, Reis DJ (1998) Regional localization of agmatine in the rat brain: an immunocytochemical study. Brain Res 787(1):1–14

Pegg AE (1986) Recent advances in the biochemistry of polyamines in eukaryotes. Biochem J 234(2):249–262

Reis DJ, Regunathan S (1998) Agmatine: a novel neurotransmitter? Adv Pharmacol 42:645–649

Reis DJ, Regunathan S (2000) Is agmatine a novel neurotransmitter in brain? Trends Pharmacol Sci 21(5):187–193

Reis DJ, Li G, Regunathan S (1995) Endogenous ligands of imidazoline receptors: classic and immunoreactive clonidine-displacing substance and agmatine. Ann N Y Acad Sci 763:295–313

Reis DJ, Yang XC, Milner TA (1998) Agmatine containing axon terminals in rat hippocampus form synapses on pyramidal cells. Neurosci Lett 250(3):185–188

Roberts JC, Grocholski BM, Kitto KF, Fairbanks CA (2005) Pharmacodynamic and pharmacokinetic studies of agmatine after spinal administration in the mouse. J Pharmacol Exp Ther 314(3):1226–1233

Sastre M, Regunathan S, Galea E, Reis DJ (1996) Agmatinase activity in rat brain: a metabolic pathway for the degradation of agmatine. J Neurochem 67(4):1761–1765

Satriano J (2003) Agmatine: at the crossroads of the arginine pathways. Ann N Y Acad Sci 1009:34–43

Satriano J (2004) Arginine pathways and the inflammatory response: interregulation of nitric oxide and polyamines: review article. Amino Acids 26(4):321–329

Satriano J, Matsufuji S, Murakami Y, Lortie MJ, Schwartz D, Kelly CJ, Hayashi S, Blantz RC (1998) Agmatine suppresses proliferation by frameshift induction of antizyme and attenuation of cellular polyamine levels. J Biol Chem 273(25):15313–15316

Van der Werf YD, Witter MP, Groenewegen HJ (2002) The intralaminar and midline nuclei of the thalamus. Anatomical and functional evidence for participation in processes of arousal and awareness. Brain Res Brain Res Rev 39(2–3):107–140

Vargiu C, Cabella C, Belliardo S, Cravanzola C, Grillo MA, Colombatto S (1999) Agmatine modulates polyamine content in hepatocytes by inducing spermidine/spermine acetyltransferase. Eur J Biochem 259(3):933–938

Winsky L, Isaacs KR, Jacobowitz DM (1996) Calretinin mRNA and immunoreactivity in the medullary reticular formation of the rat: colocalization with glutamate receptors. Brain Res 741(1–2):123–133

Zomkowski AD, Hammes L, Lin J, Calixto JB, Santos AR, Rodrigues AL (2002) Agmatine produces antidepressant-like effects in two models of depression in mice. Neuroreport 13(4):387–391